Investigation of Local Scour and Flow Field Around Bridge Pier with and Without Collar Through Numerical Simulation

Ningombam Bishwajit Singh and Thiyam Tamphasana Devi

1 Introduction

Localized scouring in the surrounding areas of a bridge pier has the potential to expose a significant portion of the erodible bed around the bridge pier. The extent of erosion could be such that the anchorage depth of the pier foundation shall not be sufficient enough to keep the structure safe leading to the failure of the bridge. Recent incidents of failure of bridges due to localized scouring have been reported in the literature. These failures suggest the need of finding reliable and effective scour protection countermeasures. Devices for scour protection are broadly classified into bed armoring and flow-altering countermeasures [1]. The flow-altering device of collar plate skirting around the pier has been experimentally studied extensively by several researchers [2–7]. Mashahir et al. [8] drew a comparison with the results of Ettema [9] and stated that a collar plate having a diameter three times the pier diameter has better efficacy than two times the pier diameter in mitigating the scour depth when placed at the level of the sediment bed. Garg et al. [7] stated that a collar having a minimum diameter of three times the collar plate can completely arrest the formation of scour when positioned at bed level. A parametric study on the use of collars by Setia et al. [10] found that a collar plate having a size of 2.5 times that of the pier diameter resulted in the reduction of scour depth by 85% as compared to scour depth around an unprotected pier.

Recent advancement in computational resources has increased the applicability of numerical simulation in the study of hydraulic structures. In previous studies, most of the researchers used the RANS model to simulate the bridge scour model. In the past few years, more advanced turbulence models like Detached Eddy Simulation (DES) and Large Eddy Simulation (LES) have also been employed in the study of localized scouring around the bridge pier. Kirkil et al. [11] investigated turbulence

N. B. Singh · T. T. Devi (✉)

Department of Civil Engineering, National Institute of Technology, Manipur 795004, India
e-mail: thiyam85@gmail.com

at a circular bridge pier using the DESturbulence model and showed the features of large-scale eddies which are responsible for the scour process. Alemi et al. [12] numerically investigated the flow behavior around a cylindrical bridge pier using the LES Smagorinsky model. Tafarojnoruz et al. [13] describe the flow pattern within the scour cavity for a submerged pile using the LES turbulence model. Chen et al. [14] introduced a new model of collar known as a hooked collar and studied both experimentally and numerically the flow field. The result shows that the maximum turbulent kinetic energy has been significantly reduced and the scour protection efficacy has been reduced to 42% when placed at the bed level.

2 Numerical Model Set up

2.1 Characteristics of Flow Domain and the Sediment Bed

The computational domain has a dimension of 2.25 m × 1 m × 0.286 m (L × B × H). A cylindrical pier of diameter 90 mm is positioned 1.08 m away from the upstream inlet in the longitudinal direction. Along the lateral direction, it is placed midway between the two lateral walls. A very mild slope of 0.1% i.e. 1 in 1000 is also maintained. The length of the domain is chosen based on the findings of Sarker [15] that the pile can influence its flow field up to a length of 12 times the pier diameter. It is also ensured that the chosen diameter of the cylindrical pier is less than 10% of the channel width to prevent the influence of lateral boundaries on the scour depth as reported in Chiew and Melville [16].

The numerical simulation is prepared for 2 types of models. The first model is for a cylindrical pier that is unprotected. In this model, the cylindrical pier has a diameter of 90 mm. The other model is the cylindrical pier protected with a collar. "Garg et al. [7] found that the use of a single collar which has a minimum diameter of 3 times the pier diameter can completely restrain the formation of scour when positioned at the level of sediment bed". "Mohammad et al. [8] and Ettema [9] stated that a collar plate whose diameter is three times the pier diameter is more efficient than the collar with twice the pier diameter in preventing the scour formation when both the collars are placed on the channel bed level". Thus, the width of the collar plate (D) is chosen to be three times the width of the pier (d). Figure 1 represents the schematic diagram of the model of the pier protected by the collar.

2.2 Sediment Scour Model

A single sediment species of diameter 0.418 mm having a density of 2650 kg/m^3 is chosen. Other parameters such as maximum packing fraction, coefficient of entrainment, bed load coefficient, and angle of repose are assumed. The prescribed
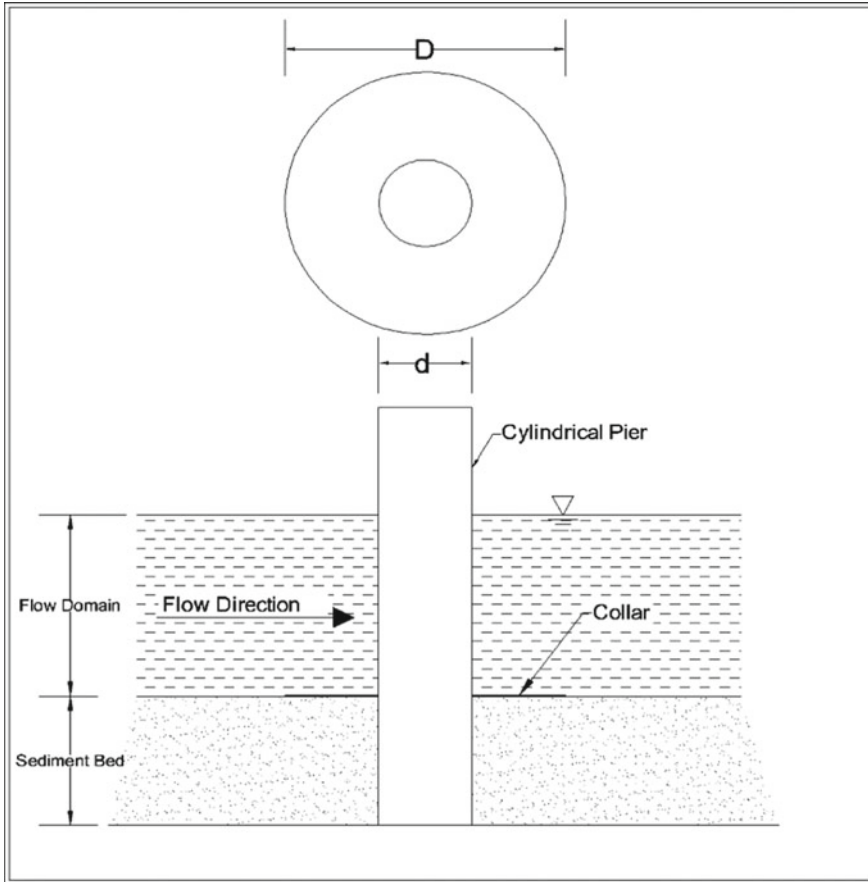
Fig. 1 Schematic diagram of collar round the cylindrical pier placed at bed level

critical Shield's number is calculated based on Soulsby-Whitehouse Equation. The dimensionless parameter d_{*i} is calculated prior to the finding of the critical Shield's parameter (Eq. 1).

$$d_* = d_i \left[\frac{\rho_f (\rho_i - \rho_f) g}{\mu_f} \right]^{1/3} \tag{1}$$

where d_* is the dimensionless diameter of sediment, d_i is the sediment diameter, ρ_f is the density of the fluid, ρ_i stands for a density of sediment species, μ_f and g represent dynamic viscosity and acceleration due to gravity respectively.

Thus, using the Soulsby White House equation provided underneath the dimensionless critical parameter is calculated as (Eq. 2).

$$\theta_{cr,i} = \frac{0.3}{1 + 1.2d_*} + 0.055\big[1 - \exp(-0.02d_*)\big] \tag{2}$$

where $\theta_{cr,i}$ represents the dimensionless critical shield parameter. The calculated values of the dimensionless diameter of sediment (d_*) and the prescribed dimensionless critical shield parameters $(\theta_{cr,i})$ are 1.057 and 0.1334.

2.3 Mesh

Mesh plays a vital role in the accurate determination of results. The time of operation of the simulation process is also dependent on the size of the cell. In order to numerically model the flow domain in three dimensions and to make good modeling of the formation of scour hole and vortices, the nested meshing technique is adopted. It is also ensured that the outer mesh cell size and the inner cell size do not differ by large value and hence aspect ratio of 1:2 is maintained. Keeping an aspect ratio of nearly 1:2 will help in minimizing the error empirically. The outer mesh block is assigned a cell size of 2 cm while the inner nested mesh block is assigned a cell size of 1 cm. The total cell count of both the larger and smaller cell size is 302658. The calculations are performed on CPU core 20 with 56 GB RAM. The large domain and the presence of a number of cells consume an enormous time of more than 48 h.

2.4 Boundary Conditions

Assigning appropriate boundary conditions to form an essential part of a numerical simulation. They are chosen in such a manner that they correspond to the physical conditions of the model. The assigned boundary conditions direct the motion of the fluid leading to the formation of a unique solution. At the inlet boundary, the boundary condition of volumetric flow rate (V_{fr}) is applied. The constant flow rate of 0.035 cumecs is set with the elevation of fluid being fixed at 0.284 m. At the outlet, the specified pressure (P) is applied with the same fluid elevation as set earlier. The topmost boundary which is the free surface is assigned as specified pressure (P) with zero fluid fraction. The two lateral sides are specified as symmetric boundaries (S). The bottom floor is set as a wall (W) which acts as a frictionless surface. In order to attain faster convergence, a constant water depth of 11.6 cm is set throughout the computational domain in the initialization stage. The applied boundary conditions are tabulated in Table 1 which is shown below. Further, we assign LES turbulence model which relies more on calculation of eddies larger than mesh cell size rather than modeling of eddies smaller than the cell size.

Table 1 Applied boundary conditions

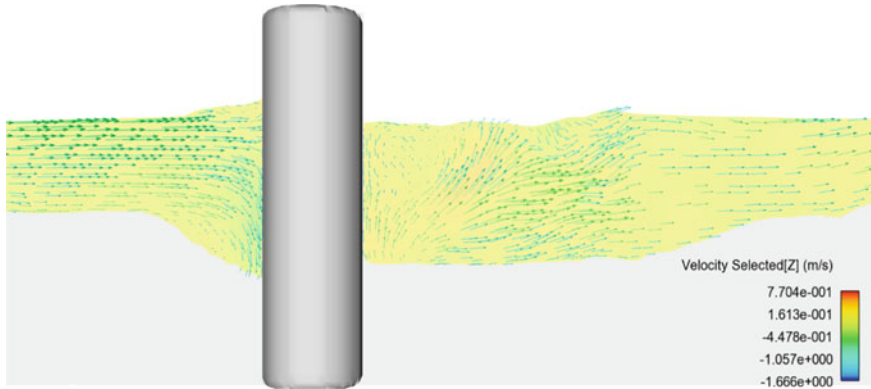| Inlet	Outlet	Lateral sides	Free surface	Bottom floor
Volumetric flow rate	Specified pressure	Symmetry	Specified pressure	Wall

3 Numerical Results

Figure 2 shows the fully developed scour cavity around the circular pier at the end of the simulation period of 1800 s. The extent of development of scour hole is almost symmetrical about the axis which is longitudinal to the direction of flow. However, the developed scour hole remains unsymmetrical about the axis which is transverse to the direction of flow as observed from the center of the pier. When gauged from the center of the pier the degree of extent of scour hole formation extends for a considerable length at the downstream portion as compared with the upstream length. The greatest extent of scour depth is recorded as high as 8.58 cm. The site of the highest scour depth is not exactly at the center of the upstream of the cylinder but is slightly shifted in the lateral direction. It is so because the scouring on areas adjacent to the pier nose is more intensive. The scour topography is in good agreement with the scour pattern of Zhu [17] which indicates that scouring is predominant beside the pier.

At the upriver of the nose of the pier, one can observe from Fig. 3 that the approaching velocity vectors decelerate to form a vertical stagnation plane. The vectors are then re-directed downwards and made to impinge on the sediment bed

Packed sediment Net Height Change Selected (m)
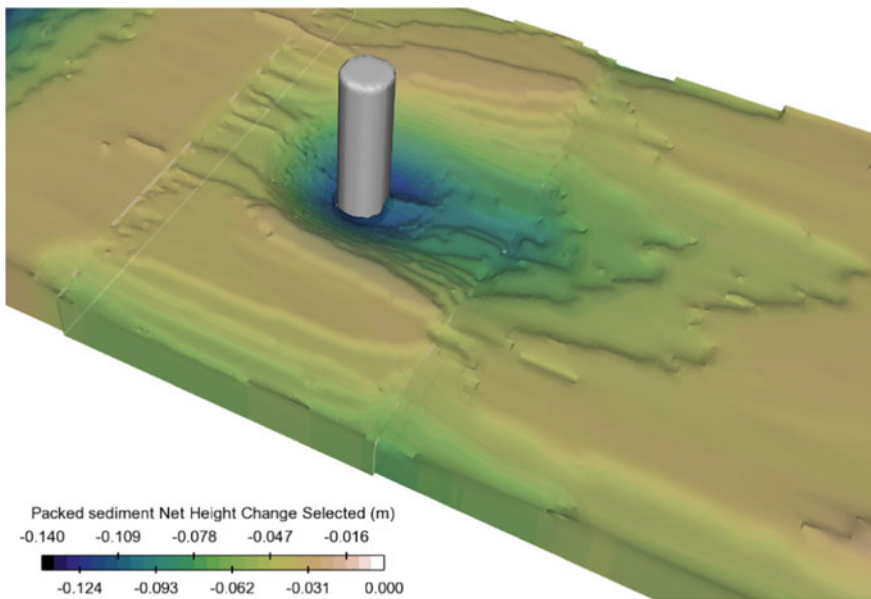
Fig. 2 Isometric view of scour hole formation around the unprotected pier

Velocity Selected[Z] (m/s)

7.704e-001
1.613e-001
-4.478e-001
-1.057e+000
-1.666e+000

Fig. 3 Velocity vectors along Z direction at the vertical symmetrical plane (y = 0.5 m)
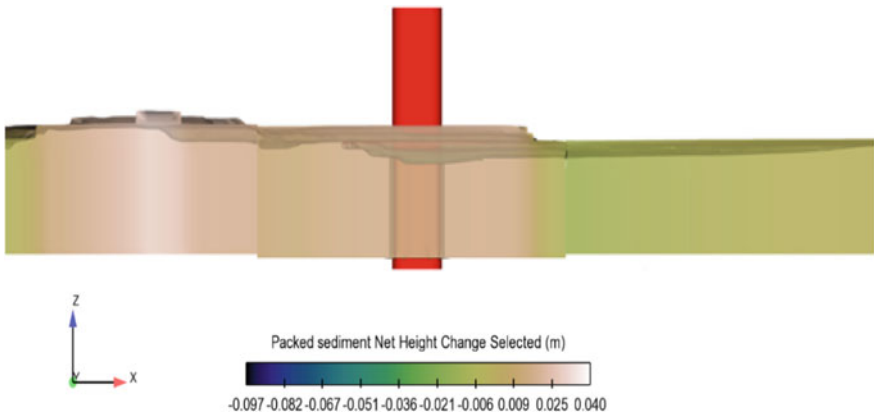
which is located underneath. This downflow induces scour development. Within the upstream scour cavity, recirculation of velocity vectors is observed which an indication that horseshoe vortices are formed is. At the downstream of the cylindrical pier, upwelling of velocity vectors is present which suggests the growth of wake vortices responsible for dislodging the eroded sediments away from the base of the pier. The above vector representation clearly indicates the mechanism of formation of the scour hole as explained by various researchers like Graf and Istiarto [18], Kothyari and Kumar [19] and Melville and Coleman [20].

Figure 4 shows the visualization of velocity vectors of the flow domain around a pier protected by a collar. The presence of the collar plate is able to shield the downward impact of downflow as it acts as an erosion-resistant surface. It is able to arrest the sinking horseshoe vortex and mitigate the growth of scour cavity around the pier. Figure 5 shows the scour cavity developed around the pier protected by collar at the end of the simulation time of 1800 s. One can observe from Fig. 5 that the depression of the scour hole is substantially reduced as weighed against the depth of scour of an unguarded pier. Furthermore, the areal extent of scour cavity developed around the cylindrical pier protected by collar plate has been notably minimized.

Figure 6 shows the plot of the change of scour depth with time. In the case of unprotected pier, the scour depth rises rapidly in the early stage of scouring. However, for the pier protected by collar, the scour depth remains more or less the same from the instant of 600 s till the end of the simulation. It indicates that scour depth has attained equilibrium. The highest recorded scour depth for the collar-protected pier is as high as 1.1 cm. Hence the effectiveness of using a collar plate as scour mitigation remedy is 87.71%. This is in good agreement with the experimental result of Setia and Shubhneet [4] which stated 85% scour protection efficacy of collar plate (2.5D) over the scour penetration of an unguarded pier. However, the obtained scour protection efficacy of 87.71% is lesser as compared to the result of Garg et al. [7] having 100% efficacy of collar (3D) when positioned at the bed level. Figure 7 illustrates the plan view of the scour cavity developed around the pier protected by the collar. The

Velocity Selected[Z] (m/s)

-0.395   -0.331   -0.266   -0.202   -0.137   -0.073   -0.008   0.056   0.121   0.186
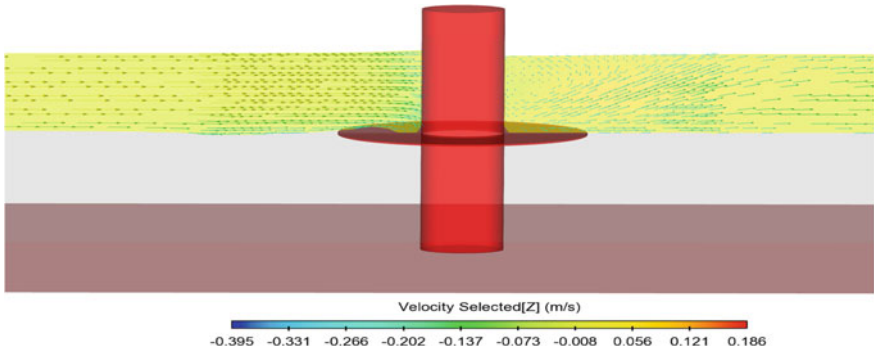
Fig. 4 Velocity vectors along Z direction at the vertical symmetrical plane (y = 0.5 m) of pier protected with collar

Packed sediment Net Height Change Selected (m)

-0.097 -0.082 -0.067 -0.051 -0.036 -0.021 -0.006 0.009 0.025 0.040

Fig. 5 Side elevation view of scour hole formation around the pier-protected collar plate

scour pattern so developed varies significantly with that of the scour pattern of the unprotected pier. One can observe that the scour is shifted radially outwards from the pier.

No scour is seen to occur at the downstream location of the pier. In the case of unprotected pier scour happens at the close surrounding area of the pier. However, for the collar-protected pier, scour is seen to occur around the periphery of the collar except at the downstream portion.
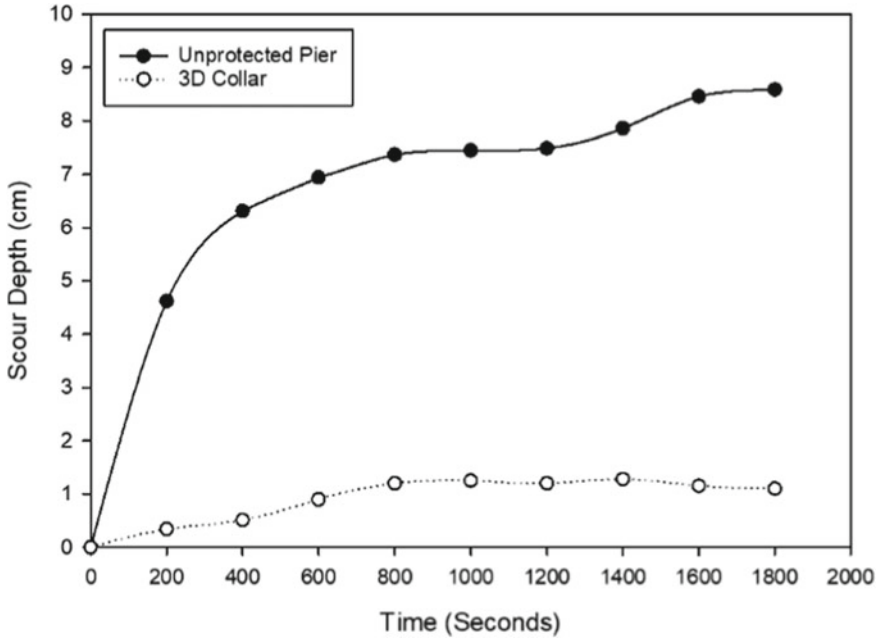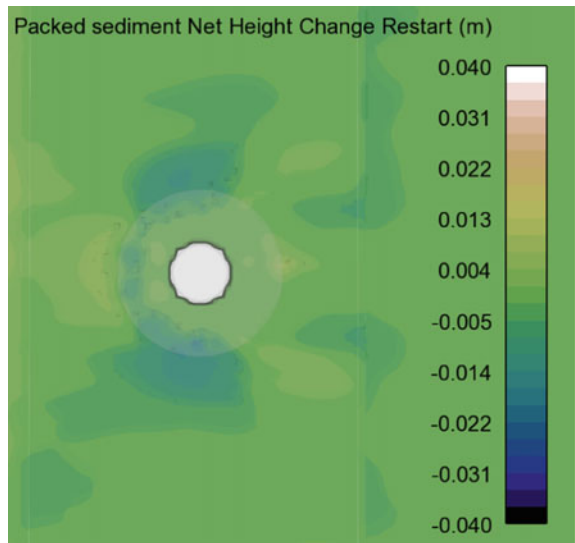
Fig. 6 Temporal change of scour depth

Fig. 7 Plan view of the scour cavity formed around the collar-protected pier

4 Conclusion

A collar plate skirting around the pier of diameter three times the pier diameter is capable of decreasing the scour depth by 87.71%. It can also be inferred that the usage of collar plate is not able to entirely remove scour when positioned at the top of the sediment bed. It is able to impede the growth of the horseshoe vortex and effectively inhibit the development of scour around the cylindrical pier. The efficacy of the collar plate will remain unaltered by variations in the direction of flow as the collar plate is symmetrical about the pier. Hence, collar plate of 3 times the pier size placed at the bed level can be effectively used to mitigate the scour formation.

References

1. Singh NB, Devi TT, Kumar B (2022) The local scour around bridge piers—a review of remedial techniques. J Hydraul Eng 28(S1):527–540. https://doi.org/10.1080/09715010.2020.1752830
2. Dargahi B (1991) Controlling mechanism of local scouring. J Hydraul Eng 116(10):1197–1214. https://doi.org/10.1061/(ASCE)0733-9429(1990)116:10(1197)
3. Chiew Y (1992) Scour protection at bridge piers. J Hydraul Eng 118(9):1260–1269. https://doi.org/10.1061/(ASCE)0733-9429(1992)118:9(1260)
4. Setia B (1997) Scour around bridge piers: mechanism and protection. Dissertation, Department of Civil Engineering, Indian Institute of Technology, Kanpur, India
5. Kumar V, Raju KGR, Vittal N (1999) Reduction of local scour around bridge piers using slots and collars. J Hydraul Eng 125(12):1302–1305. https://doi.org/10.1061/(ASCE)0733-9429(1999)125:12(1302)
6. Kim UY, Kim JS, Ahn SJ, Hahm CH (2005) Scour countermeasure using additional facility in front of bridge pier. In: 31st IAHR congress 2005: water engineering for the future, choices and challenges. Seoul, pp 5823–5829
7. Garg V, Setia B, Verma DVS (2005) Reduction of scour around a bridge pier by multiple collar plates. J Hydraul Eng 11(3):66–80. https://doi.org/10.1080/09715010.2005.10514802
8. Mashahir MB, Zarrati AR, Rezayi MJ (2004) Time development of scouring around a bridge pier protected by collar. In: 2nd International conference on scour and erosion, Meritus Mnadarin, Singapore
9. Ettema R (1980) Scour at bridge piers. Dissertation, Department of Civil Engineering, University of Auckland, New Zealand
10. Setia BS (2016) Scour protection by collar plates: a parametric study. In: Proceedings of the international conference on fluvial hydraulics, river flow, pp 486–494
11. Kirkil G, Constantinescu G, Ettema R (2009) Detached Eddy simulation investigation of turbulence at a circular pier with scour hole. J Hydraul Eng 135(11):888–901. https://doi.org/10.1061/(ASCE)HY.1943-7900.0000101
12. Alemi M, Pêgo JP, Maia R (2017) Numerical investigation of the flow behavior around a single cylinder using large Eddy Simulation model. Ocean Eng 145:464–478. https://doi.org/10.1016/j.oceaneng.2017.09.030
13. Tafarojnoruz A, Lauria A (2020) Large eddy simulation of the turbulent flow field around a submerged pile within a scour hole under current condition. Coast Eng J 62(4):489–503. https://doi.org/10.1080/21664250.2020.1807453
14. Chen SC, Tfwala S, Wu TY, Chan HC, Chou HT (2018) A hooked-collar for bridge piers protection: flow fields and scour. Water 10(9):1–12. https://doi.org/10.1080/21664250.2020.1807453

15. Sarker M (1998) Flow measurement around scoured bridge piers using acoustic-Doppler velocimeter (ADV). Flow Meas Instrum 9(4):217–227. https://doi.org/10.1016/S0955-5986(98)00028-4
16. Chiew YM, Melville BW (1987) Local scour around bridge piers. J Hydraul Res 25(1):15–26
17. Zhu ZW, Liu ZQ (2012) CFD prediction of local scour hole around bridge piers. J Cent South Univ Technol 19(1):273–281. https://doi.org/10.1007/s11771-012-1001-x
18. Graf WH, Istiarto I (2002) Flow pattern in the scour hole around a cylinder. J Hydraul Res 40(1):13–20. https://doi.org/10.1080/00221680209499869
19. Kothyari UC, Kumar A (2010) Temporal variation of scour around circular bridge piers. ISH J Hydraul Eng 16:35–48. https://doi.org/10.1061/(ASCE)0733-9429(1992)118:8(1091)
20. Melville BW, Coleman SE (2000) Bridge scour. Water Resources, LLC, CO, USA